geosciences

Article

Geoacoustic Digital Model for the Sea of Japan Shelf (Peter the Great Bay)

Aleksandr Samchenko *, Grigory Dolgikh, Igor Yaroshchuk, Roman Korotchenko and Alexandra Kosheleva

V.I. Il'ichev Pacific Oceanological Institute Russian Academy of Sciences, 43 Baltiyskaya Str., Vladivostok 690041, Russia; dolgikh@poi.dvo.ru (G.D.); yaroshchuk@poi.dvo.ru (I.Y.); korotchenko@poi.dvo.ru (R.K.); kosheleva@poi.dvo.ru (A.K.)

* Correspondence: samchenco@poi.dvo.ru; Tel.: +7(914)-682-6697

Abstract: In this paper, the authors present and analyze the geoacoustic digital seabed model they developed, which is a digital description of the water column characteristics, seabed topography, and information about sediments and rocks (their composition and elastic properties) for Peter the Great Bay, the Sea of Japan. The model consists of four relief layers, a foundation and three layers of bottom sediments, and also contains the velocities of longitudinal waves in rocks and statistical characteristics of the sound velocity distribution in the water layer for three seasons. Acoustic characteristics of geological structures are based on seismoacoustic studies, sediment lithology, and laboratory measurements of rock samples collected onshore. The velocities of longitudinal and transversal waves and also the density of the sediments were calculated from their empirical dependencies on the granulometric composition of bottom sediment samples over an area of about 800 km^2. In a limited area of the shelf (approximately 130 km^2), high-frequency acoustic studies were carried out using echo sounders, and the longitudinal wave velocities of the top sedimentary layer were determined. Porosity, density, longitudinal, and transverse wave velocities in bottom sediments were calculated using empirical models with a normal coefficient of reflection from the seabed. A comparison was made of the results of calculating the elastic properties of the seabed using various methods.

Keywords: relief; digital terrain model; geoacoustic digital model; singular spectral analysis; Peter the Great Bay

Citation: Samchenko, A.; Dolgikh, G.; Yaroshchuk, I.; Korotchenko, R.; Kosheleva, A. Geoacoustic Digital Model for the Sea of Japan Shelf (Peter the Great Bay). *Geosciences* **2024**, *14*, 288. https://doi.org/10.3390/geosciences14110288

Academic Editor: Luciano Telesca

Received: 28 August 2024
Revised: 24 October 2024
Accepted: 25 October 2024
Published: 28 October 2024

1. Introduction

The Geoacoustic Digital Model (GADM) of a shelf area is a special case of 3D geological modeling and is designed to study the propagation of seismoacoustic and hydroacoustic signals. The description, principles of creation, and purpose of the geoacoustic model are presented in the work of Hamilton [1]. The relevance of the GADM in geological media does not decrease; on the contrary, methods and approaches to its creation continue to be improved [2–7]. In the paper [8], the authors determine the characteristics of bottom sediments and evaluate their changes over time. A number of software products have been developed for digital modeling of the lithology of geological media, for example, 3D GeoModeller, GeoScene3D, Leapfrog 3D, Oasis montaj Geosoft, RockWorks, GeoStudio, etc. [9–11].

Three-dimensional digital models are in demand for interpreting many field observations in scientific, economic, and industrial research [12].

To interpret the results of observations on oscillations' propagation on the shelf, it is necessary to solve the following problem: to select an extended geo-hydroacoustic digital model for subsequent analysis of seismic and hydroacoustic parameters in the shallow water area. Therefore, modeling only the geological media with standard programs is insufficient when modeling the propagation of seismoacoustic signals. This paper proposes some solutions for creating a digital model, the results of which can be adapted for any geoinformational media.

When solving problems of low-frequency hydroacoustic modeling, and also when interpreting the results of seismoacoustic experimental observations, it is necessary to have a general understanding of the parameters and properties of acoustic paths [13,14]. In the case of using low-frequency signals, both the water layer and the top seabed layer serve as the acoustic path. The authors conduct research on the propagation of acoustic signals along paths that are spatially inhomogeneous, for example [15]. Lithological heterogeneity along the path leads to the fact that in the study area along one of the profiles, the change in the velocity of a longitudinal wave (*P*-wave) can be more than 100 m/s per 2–3 km. This happens, for example, when moving to the outer edge of the bay, where the depth dump begins. Therefore, the GADM for a shelf test site has important practical significance.

In the generally accepted understanding, the GADM of a shelf zone describes the water layer, the sedimentary stratum consisting of loose and consolidated sediments, and the solid foundation [1,16]. It has different aspects of presentation—qualitative, descriptive, and quantitative, in which all characteristics are formalized in the form of space–time dependencies. The transition from descriptive to quantitative characteristics of the medium occurs through the accumulation and processing of experimental data and laboratory research results. To create a GADM of the sedimentary layer and foundation, it is necessary to have a general understanding of the geological structure of the study area.

The Digital Terrain Model (DTM) is the basis of a digital geoacoustic model. Various methods and approaches are used in the construction of a DTM [17,18]. In our work, it is presented as a set of surfaces with elevation characteristics corresponding to various geomorphological structures. A DTM is built by combining the Natural Neighbor Interpolation (NNI) standard method [19] and the two-dimensional singular spectral analysis (2D–SSA) method [20,21]. An important factor is the appearance of distortions and artifacts, especially in transition zones. For example, in our case, they appear in the area of the coastline ("water-land" transition), where there are not enough real measured values, and also in cases of sharp relief gradients. Distortions along the coastline and sudden vertical changes in relief are localized due to the properties of the NNI method.

There are two approaches to determining the elastic properties of the seabed—direct and indirect. The direct approach to obtain elastic characteristics is to measure them on samples of bottom sediments or using empirical dependencies. Let us consider some direct methods for determining elastic characteristics. In one of the variants of recalculating the acoustic characteristics of bottom sediments, models of heterogeneous (porous fluid-saturated) media are currently used—the Bio–Stoll poroelastic theory, the suspension model, and some other models, which are a generalization of the theory of elasticity to multiphase media [22–24]. Evaluation of a Poroelastic Seabed Model is given in [25]. Formed as a separate area of research on the porous structure of sediments, the Bio–Stoll model is often used in research even at the present time [26]. The work [27] shows the dependence of acoustic characteristics on the granulometric and chemical composition of bottom sediment samples. In the Bio–Stoll model, bottom sediments are represented as a two-phase quasi-equilibrium system, where a rigid skeleton formed by many contacting solid particles is saturated with liquid. The presence of gas bubbles in sediments can have a significant influence. These models for calculating the acoustic characteristics of loose bottom sediments imply serious requirements for sediment sampling and laboratory research. To create such models, it is almost impossible to carry out all laboratory measurements on previously collected samples, while the granulometric and chemical composition of bottom sediment samples can be re-checked.

A simpler method for determining elastic properties was proposed by Hamilton and Bachman [16]. The method is based on obtaining empirical dependencies of the elastic properties of bottom sediments on their granulometric composition. An important advantage of this method is that it is possible to use an extensive database of previously studied sediment samples and to carry out their verification. However, it has lower accuracy for determining the properties of sediments.

Seismoacoustic methods [28–30] can be related to indirect methods for determining the elastic properties of bottom sediments. A method of inversion of the properties of marine sediments based on the measured normal coefficient of reflection based on the full Bio–Stoll theory and analytical solutions applied to a rigid skeleton filled with liquid is used. Its simplified version [31] uses only viscous friction.

The simulated area is located in the shelf zone of Peter the Great Bay of the Sea of Japan and also includes the coastal part of the land. The choice in the shelf area, for which the GADM was developed, is due to the fact that it includes the hydrophysical test site of V.I. Il'ichev Pacific Oceanological Institute, where the institute's staff systematically conduct various acoustic studies, hydrological measurements, and seismoacoustic experiments [32,33].

This paper is structured as follows: Section 2 provides a description and structure of GADM; Section 3 describes methods and approaches to forming a model of surfaces (the seabed and other geological layers). Section 4 describes the formation of the GADM based on the created DTM by filling it with acoustic parameters of the media and characteristics of the water layer taken from the averaged data of long-term hydrological and hydrographic measurements.

2. Geoacoustic Digital Model

The typical geological structure of the shelf of the Russian Far Eastern seas is characterized by rather abrupt spatial changes in the structure and physical properties of rocks. Fault zones, shifts, faults in bedrock can be traced in the land and water areas; sedimentary layers have different physical properties, which depend on the type of rocks and their granulometric composition. In loose sedimentary layers, lenses, and interlayers with acoustic parameters that differ from the host rocks are observed. The GADM is used to clarify the geological structure of the shelf and to determine the physical characteristics of the media.

This paper shows an example of the adaptive application of geological and geophysical information to the formation of a GADM on a specific shelf site based on research [1]. The digital model was built as a result of processing natural data from hydroacoustic, seismoacoustic, and geological studies obtained with the participation of the authors of this paper. Information about the geological structure of the region was taken from [34–36]. To develop a GADM for the shelf area, available data on the granulometric composition of the top layer of sediments and topography of Peter the Great Bay area were used. The model can be significantly improved by supplementing the existing fragmentary geological and geophysical data with data from drilling and through expanding the geography of seismic research.

When creating the GADM of the shelf area, analytical solutions were used to calculate the acoustic parameters of loose bottom sediments based on their granulometric composition with similar chemical composition [37]. The constructed model of the site lithology took into account the compaction of loose sediments with depth in accordance with the studies described in [38,39]. This approach is not modern, but it is quite simple and universal. The adequacy of the GADM to the natural situation was tested on a small area using acoustic methods. The development concept based on Hamilton's research was determined by the following factors:

- The unification of GADM allows, based on already obtained analytical solutions, to recalculate the acoustic characteristics of bottom sediments;
- We can use data on the granulometric composition of loose bottom sediments from all previously conducted studies in the water area of interest, which allows us to expand GADM to large areas.

The hydrophysical test site of the POI FEB RAS is located in the bay [32,33] (Figure 1). The authors have been actively conducting hydroacoustic and oceanological research on it for fifteen years [40,41].

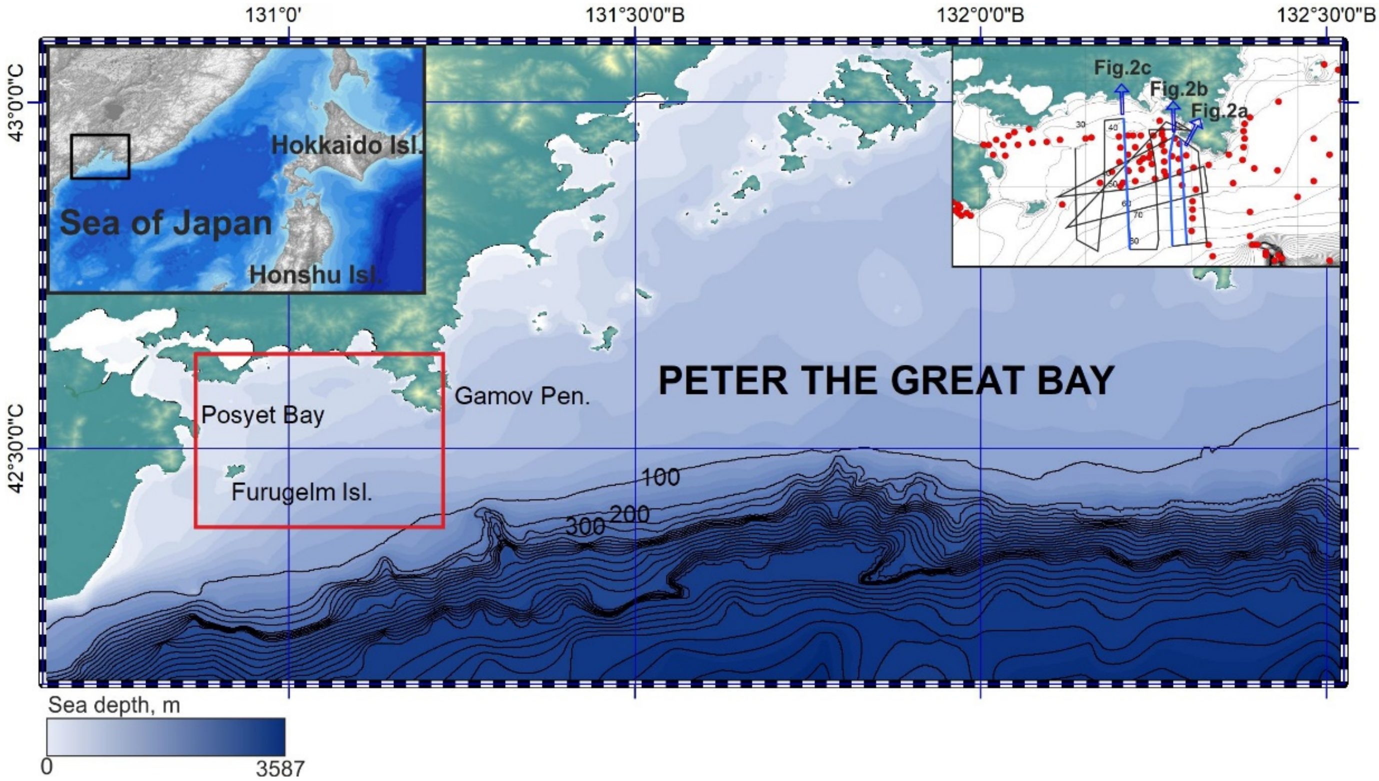

Figure 1. Peter the Great Bay; its location on the Sea of Japan map is shown in the upper left corner. Red rectangle shows the shelf area under study. The upper right corner shows a map with sediment sampling points (red dots) and seismoacoustic and bathymetric surveys (black and blue lines). Blue lines indicate the routes, the profiling results of which are shown in Figure 2a–c.

Geological and geophysical studies were also carried out in this area [42]. The right inset in Figure 1 shows sediment sampling points and the routes of seismoacoustic surveys. Profiles obtained along three of these routes (marked in blue on the inset in Figure 1) are presented in Figure 2. The study of the acoustic characteristics of the water column and geological formations in the waters of Peter the Great Bay provides an improved interpretation of the results of the hydrophysical and geophysical studies carried out on the shelf area under study. The GADM allowed us to trace some patterns of propagation of acoustic signals depending on the conditions of the sedimentary layer formation.

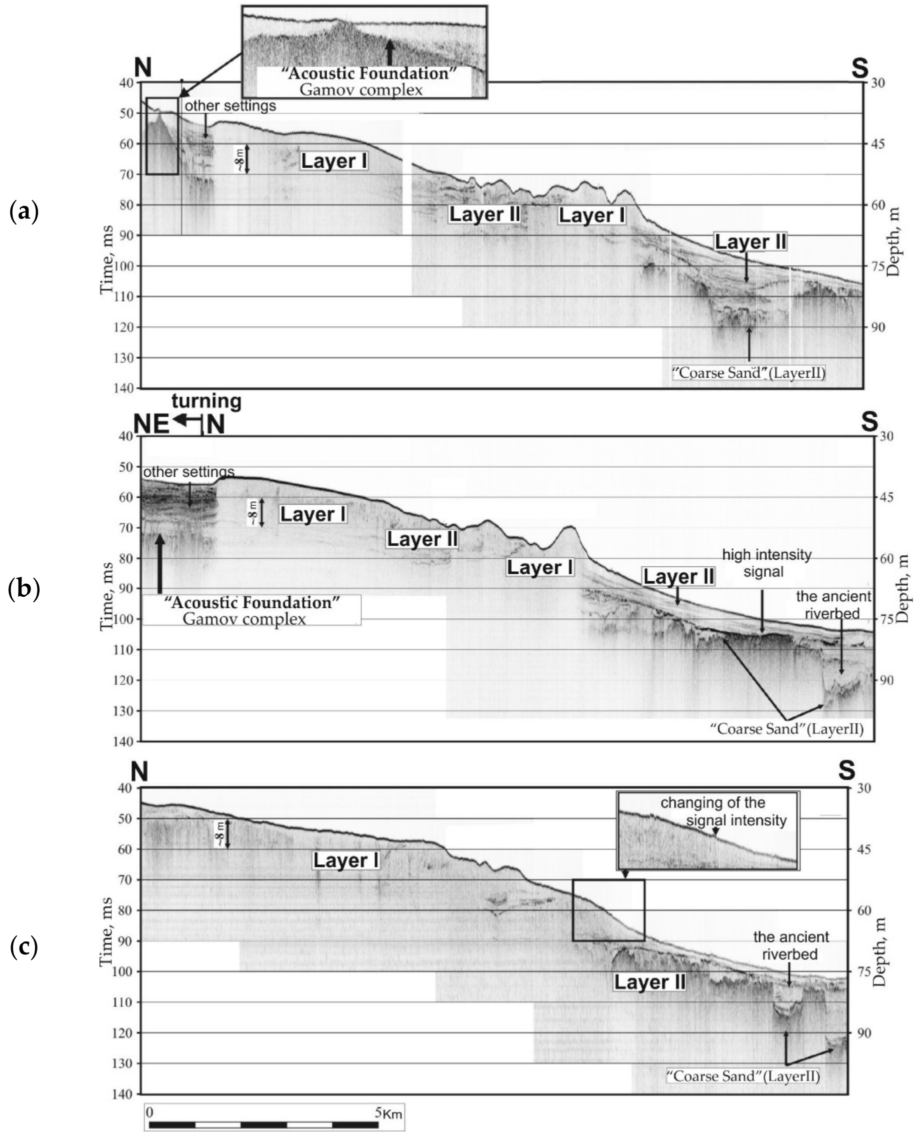

Figure 2. (**a**–**c**) Seismoacoustic profiles corresponding to the routes marked in Figure 1. Letters S, N, and NE indicate south, north, and northeast, respectively. The ordinate axis represents the two-way travel time of the wave.

3. Digital Terrain Model

3.1. Methods and Approaches

Creating a DTM of all layers of geological structures was carried out by the authors in two stages. At the first stage, using the NNI standard algorithm, we processed field observations and electronic data from GEBCO, ASTER (for the seabed and land) into the primary DTM with a cell size of 0.056 $\times$ 0.04 km. In the NNI method, the value of the variable depth (z) at some point in the study area was taken as the value of the nearest point selected in terms of Euclidean distance. This method was used because it works well when superimposing field measurements onto a regular grid of global electronic seabed bathymetry data. However, in areas between the coastline and field data receiving points, outliers and artifacts may appear on the detailed grid and must be taken into account. In addition, the NNI method allows us to fix the local area where we have data gaps in field measurements. The interpolation happens by finding the closest subset of input samples to the requested point and applying to them weights based on proportional regions [19]:

$$G(x,y) = \sum_{i=1}^{N} \omega_i f(x_i, y_i), \quad (1)$$

where $G(x, y)$ is the desired value; (x_i, y_i) are measured values; N is the dimension of the space; ω_i are weight coefficients.

To solve the problem of smoothing and filtering noise in the DTM, the 2D–SSA method was applied in the second stage. This method is part of a more general methodology of natural (empirical) orthogonal functions (EOFs) for processing natural data [20,21]. An EOF is one of the most popular tools in meteorology and atmosphere and ocean physics. The main idea behind the method is as follows. Let us assume that the implementations of data fields are represented by a set of vectors $\{f_i, i = 1...k\}$ in N–dimensional space for a sequence of moments in time. All vectors come out from the coordinates' origin. If the source data is correlated, the vectors will be clustered along some selected directions. The task of the EOF method is to find such an orthogonal basis $\{e_1, e_2, \ldots, e_N\}$ in N–dimensional space that the vector e1 is directed towards the largest cluster, vector e_2–to the next largest, etc. In this case, the sum of the squares of the projections of all vectors f onto the directions $\{e_1, e_2, \ldots, e_N\}$ decreases strictly consistently. Due to the orthogonality of the vectors $\{e_1, e_2, \ldots, e_N\}$, the found structures are called orthogonal functions. And since the new basis is constructed from the data and is not chosen a priori, these functions are called natural or empirical. From an applied point of view, the key factor is the possibility of selecting an orthogonal basis, constructed by the data itself and arranged so that the "layout" of the initial data in the basis is consistent in descending order of contribution to the overall maximum variation. This means that the EOF splits the original data fields into orthogonal components that describe statistically significant, orderly structures.

The 2D–SSA method is one of the varieties of the EOF method, offering additional advantages, where the most important thing is the stability of the analysis results in relation to the choice of averaging parameters during processing. The principles and details of the algorithm are described in [20].

The SSA algorithm includes two stages: decomposition and reconstruction. The parameters of the algorithm for a two-dimensional spatial field are the dimensions of the smoothing window by a moving average (n, m). Decomposition in the framework of this study involves "splitting" the relief field into spatial structures and measuring the relative contribution of each structure to the relief. The natural relationship between the amplitudes of variations of the selected relief elements and the energy scales of natural tectonic processes determines the adequacy and interpretability of the applied mathematical apparatus.

The reconstruction stage involves the selection of a limited set of eigenmodes as a basis for the formation of a digital relief model and further interpretation of the selected components as the results of natural processes of different scales in surface geomorphology and filtering of "noise" components.

The effectiveness and adequacy of the singular value analysis method for a digital model in our situation are confirmed by the following result. The 2D–SSA method compresses and smooths the DTM by using the first four modes, which contribute 89% of the calculated eigenvalues to the total variation. If we use the first 10 modes, then the total relative contribution from the eigenvalues to the total variation is 96%. Terrain components from higher decomposition modes contributed 4% in total; they were considered "noise levels" and filtered out.

3.2. Sedimentary Layers and Acoustic Foundation with DTM

The outer surface of the first sedimentary layer corresponds to the seabed. Bathymetric data was obtained using a GPS-equipped double-beam echo sounder at frequencies of 50 and 100 kHz and a seismoacoustic profiler "GeoPulse Subbottom Profiler" (GeoAcoustics, Norfolk, UK) at a frequency of 3.5 kHz (Figure 2). Approximately 230 km of profiles were completed in the study area, and more than 15,000 depth points were obtained. Field measurements data were superimposed on a uniform GEBCO (version 2019 Esri ASCII) electronic data grid (https://download.gebco.net/ (accessed on 15 August 2024)) and limited by the coastline. In the DTM, construction of the outer surface of the first sedimentary layer was carried out in two stages. In the first stage, we used the NNI method and then carried out smoothing using 2D–SSA. For the seabed, we left the first 10 decomposition modes since the detailing of the field data allows this. In addition, it can be useful when modeling the propagation of acoustic signals with frequencies greater than 100 Hz. Figure 2 shows the visual difference between smoothing by the first 10 modes (Figure 3a) and by the first 4 modes (Figure 3b) of 2D–SSA for the DTM of the seabed section. In addition, at the output of the DTM after smoothing by the 2D–SSA method, the cell size increases from 0.056 × 0.04 km to 0.15 × 0.2 km for high-frequency modeling. Since the GADM does not require greater detailing, we have reduced the DTM relief detailing down to 0.45 × 0.3 km. Thus, the number of site depth values (cells), which are then used in the digital model, for the entire studied area of the bay bottom is more than 5800. In the GADM, the coordinates of each cell are assigned a set of physical parameters [x_i, y_j, z_k] → [V_p, V_s, g, η], where V_p is the longitudinal wave velocity, V_s is the transverse wave (*S*–wave) velocity, g is the density, and η is the attenuation coefficient. The GADM is spatially limited by the bottom layer—the "acoustic foundation". The formation of the fields of geological media physical parameters will be described below.

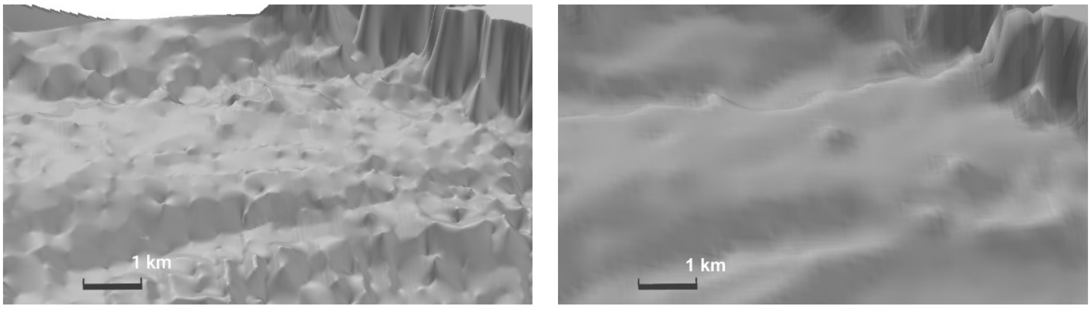

(**a**) (**b**)

Figure 3. DTM of the seabed section in monochrome visualization, (**a**) the first 10 modes, (**b**) the first 4 modes. The ratio of the relief height to the horizontal scale is 0.001.

The relief of the study area is a slightly hilly surface in the form of a sea-flooded plain, which has preserved the relics of a river valley with terraces. The southeastern stretch of the main slope determines the main scale. Depths vary from 20–30 m in the central part to 60–80 m at the southern boundary of the study area in Peter the Great Bay. The uniformity of deepening is complicated by shallow gullies and separate hills. The site is well-consistent with geographic coordinates: Its isolines are close to the latitudinal strike. The structures are elongated from northwest to southeast and have heights of about 10 m. The largest formations are an underwater hill 8–10 m high and a depression in the central part of the bay. At the exit, several small hills up to 10 m high are located in the form of arcs. In the western and southwestern parts of the site, individual structures are less noticeable.

The DTMs of two underlying sedimentary layers and the acoustic foundation were built based on data from seismic research carried out to assess the oil and gas potential of the area. The structure of the top sedimentary layer was clarified in a number of expeditions conducted by POI FEB RAS [34,42,43]. The foundation and geological sections in the studied shelf area are presented in Figures 4 and 5.

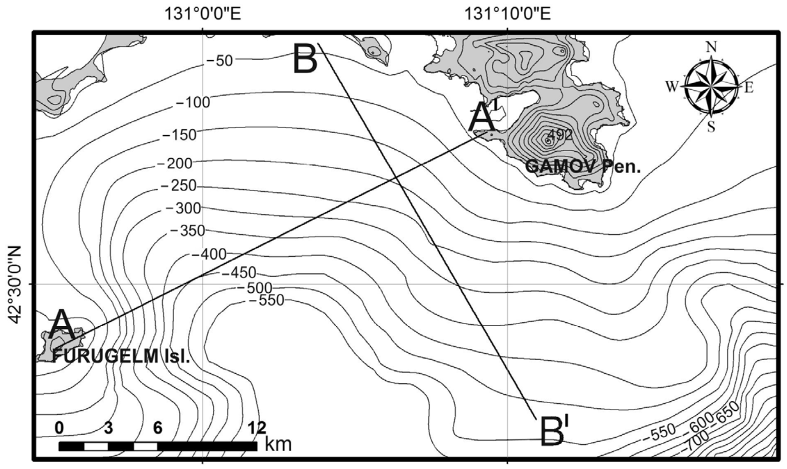

Figure 4. Boundary of the acoustic foundation bedding in the study area. AA^{I} and BB^{I} are geological sections. The sea level is taken as the zero reference level.

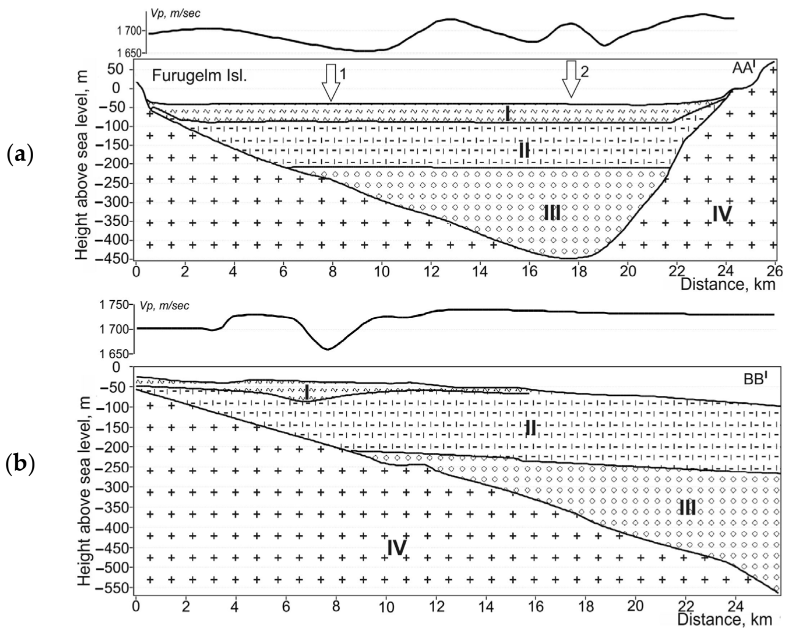

Figure 5. Geological sections: (**a**) AA^{I} and (**b**) BB^{I} shown in Figure 3. Change in the velocity of a longitudinal wave on the surface along the geological section. Layers I, II, and III indicate sedimentary deposits: medium-grained, coarse-grained, and conglomerates, respectively. Layer IV represents granites of the Gamov complex.

4. Acoustic Parameters of the Hydroacoustic Model

4.1. Water Layer

Acoustic parameters of the water layer were obtained from long-term seasonal measurements collected into a database of hydrological parameters in Peter the Great Bay [40]. In spring, summer, and autumn, using anchored thermostrings, long-term (about 2 weeks) measurements of the water layer temperature are carried out, supplemented by periodic CTD measurements [41]. A total of five to eight thermostrings are used simultaneously, distributed over the area of the study site at depths of 40–80 m. The model presents the minimum and maximum values of the physical parameters of water from the surface to the bottom, which were measured in different seasons, and extended to the entire site. An example is shown in Figure 6. Thus, in the model, the parameters change only depending on the depth of the place (Figure 5a). Complete data are presented at depths of more than 70 m; the rest are cut off by depth.

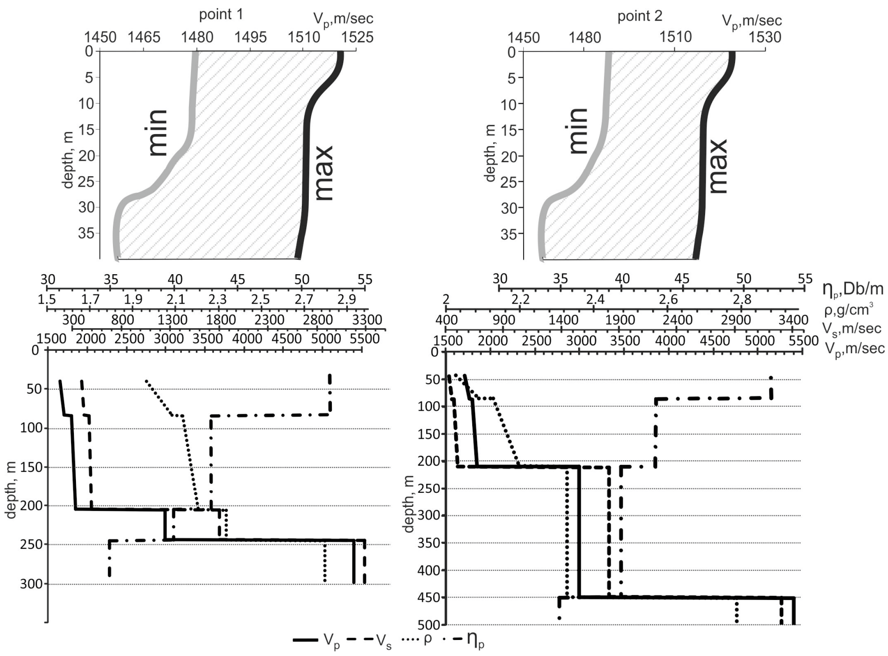

Figure 6. Variation of acoustic characteristics in GADM with depth in two points shown on geological section AAI (marked with arrows in Figure 5). *Vp*—velocity of longitudinal waves; *Vs*—transverse waves; ρ—density; η—absorption of acoustic waves.

4.2. Loose Bottom Sediments

Loose bottom sediments in the GADM are represented by the following characteristics: longitudinal and transverse wave velocities, sound absorption, and density of sediments (Figure 6). Ideally, the above characteristics of the medium are determined in the laboratory on samples, but this type of data is very scarce. We should note that all elastic properties of materials depend on each other. If we calculate the velocity of longitudinal waves V_p in loose bottom sediments, we can calculate the velocity of the transverse waves V_s, density, and other characteristics. In GADM, transverse wave velocities in loose sediments are determined based on analytical solutions presented in [37]. Density is calculated based on [1,38]. There is no direct relationship between the absorption of acoustic waves in bottom sediments (η, dB/m for 100 kHz) and the velocity of the longitudinal wave [44]. Laboratory measurements of the absorption of acoustic waves by sediments in the bay have not been carried out; the datasets were obtained based on reference data on the known granulometric composition of loose sediment samples. Therefore, the absorption of acoustic waves was set equal to the average value for the entire rock layer and is presented in Table 1.

Research conducted by Hamilton [1,37] showed that the longitudinal speed of sound is mainly affected by the size of particles in bottom sediments at equal values of watering and depth. This indicates the need to take into account the percentage of each of the fractions included in the sample. The international classification distinguishes three fractions, differing in grain size—"Sand", "Silt", and "Clay". The longitudinal speed of sound for bottom sediments with different percentages of fractions is obtained using the following relationship:

$$V_p = k_1 L_1 + k_2 L_2 + k_3 L_3, \tag{2}$$

where L_1, L_2, L_3 are the proportional content of the sand, silt, and clay fractions, respectively, in the bottom sediments sample; k_1, k_2, k_3 are appropriate coefficients, which depend on the chemical composition of the samples and are calculated on samples of similar composition. In our case, taking into account the grain size of the "Sand" fraction, the coefficients are k_1 = 1836 m/s, k_2 = 1610 m/s, with different grain sizes of the "Clay" fraction, k_3 = 1450 m/s. The longitudinal speed of sound for the option where the fraction is predominantly "Sand" will be 1750 m/s, taking into account that the grain size is on average 2.5φ units, with the fraction content predominantly "Silt"–1560 m/s for 5.4φ units (grain size in φ units = $-\log_2$ [grain size in mm]) and for 100% content of the "Clay" fraction in the sediment with a grain size of 8.5φ units—1450 m/s. When the grain size of coarse sand is 0.98φ units, the longitudinal speed of sound is 1836 m/s. The longitudinal speed of sound for the "Clay" fraction, with an average grain size of 4.5φ units, is 1610 m/s.

Table 1. Measured average acoustic properties of rock samples collected at the acoustic test site.

Rock Type	ρ, g/cm^3	V_p, m/s	V_s, m/s	η, dB/m
Coarse sand	2.08	1752	443	43.1
Medium sand	2	1690	414	47.3
Fine-grained sand	1.926	1684	411	52.1
Very fine-grained sand	1.938	1667	403	55.9
Silted sand	1.86	1619	356	74.3
Silt	1.65	1550	140	-
Conglomerates	2.33	3000	1813	-
Granites	2.79	5400	3300	35

In total, 462 samples of bottom sediments with known granulometric composition were analyzed throughout the entire territory of Peter the Great Bay, and their elastic characteristics were calculated. The calculated values of the elastic properties of the bottom sediments of Peter the Great Bay formed the basis of the created geoacoustic model. At the acoustic test site, a total of 53 bottom sediment samples were analyzed, 12 of which were collected and analyzed by the authors (Figure 7a). The values of the 2D field of the longitudinal speed of sound at the acoustic test site were calculated using the standard NNI method and are presented in Figure 7b.

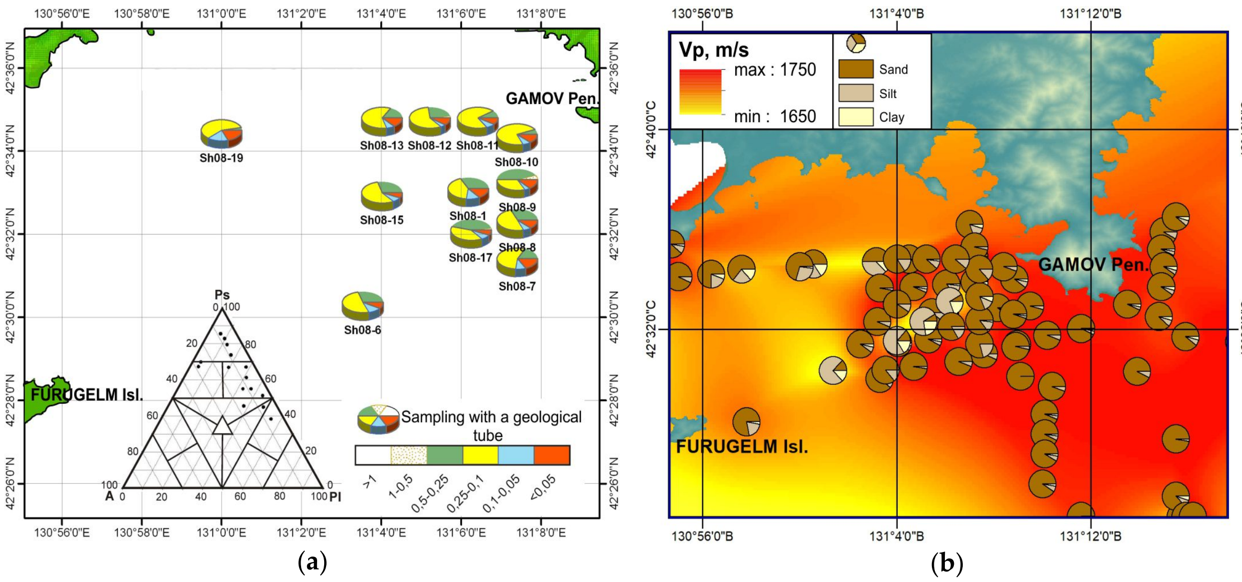

Figure 7. (**a**) Samples of bottom sediments (pie charts); (**b**) field of longitudinal wave velocity calculated from data on sediment granulometric composition; granulometric composition in the points of bottom sediments' sampling (pie charts).

In the area of about 130 km^2, acoustic testing was carried out at the acoustic test site using two frequency echo sounders. As a result of the acoustic measurements, datasets on the intensity of the backscattering at the normal beam incidence at frequencies of 50 and 100 kHz were obtained. There is a relationship between the properties of bottom sediments and reflectivity through the Rayleigh reflection coefficient:

$$R = \frac{\rho_1\rho_2 - \sqrt{C_1^2C_2^2 - \sin^2\theta}\left(\sqrt{1-\sin^2\theta}\right)^{-1}}{\rho_1\rho_2 + \sqrt{C_1^2C_2^2 - \sin^2\theta}\left(\sqrt{1-\sin^2\theta}\right)^{-1}}, \quad (3)$$

where R is the ratio of the amplitude of the reflected wave to the amplitude of the incident wave, ρ_1 and C_1 are the density and sound velocity in near-bottom water, ρ_2 and C_2 are the density and sound velocity in sediments, and θ is the angle of reflection or incidence. Figure 7 shows the calculated distribution of longitudinal wave velocities in the top layer of the bottom sediments from known data on reflective properties based on the Bio–Stoll model [23,24]. The effective density of loose sediments in the high-frequency region is calculated by the following expression [45]:

$$\rho_{eff} = \rho_f \frac{\alpha(1-\beta)\rho_s + \beta(\alpha-1)\rho_f}{\beta(1-\beta)\rho_s + (\alpha - 2\beta + \beta^2)\rho_f}, \quad (4)$$

where ρ_f is the water density and is set as 1000 $\mathrm{kg/m^3}$; ρ_s is the density of the sand grains that make up bottom sediments, corresponding to 2650 $\mathrm{kg/m^3}$ for siltstone sand; α is the permeability of the medium and can be defined as 1/25–1/15 of the average diameter of sand grains; β is porosity. For the calculation, porosity was taken equal to 0.4.

According to [31,46], if we exclude permeability but take into account the internal friction in loose sediments in Formula (4), we obtain the effective density, which is used in calculating the reflection coefficient at normal incidence using Formula (3). The magnitude of the longitudinal wave velocity in this case is not real but complex, whereas the density of bottom sediments is the effective density of a two-phase medium. Using this methodology for calculating the velocities of longitudinal waves of the top layer of bottom sediments based on acoustic–sounding data, we obtain a qualitative picture that does not differ from the calculation by the Bio–Stoll model (Figure 8). More than 150 km of profiles were surveyed using acoustic methods in the study area. The range of longitudinal wave velocities has decreased by 80 m/s: The minimum value of the longitudinal wave velocity decreased by 20 m/s and the maximum—by 60 m/s.

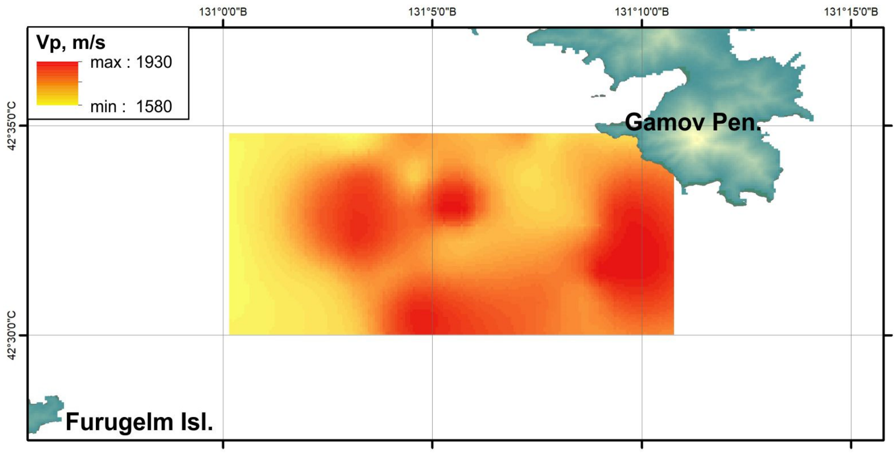

Figure 8. Longitudinal wave velocity distribution calculated from acoustic research data.

As studies at the acoustic test site have shown, the closest values of longitudinal wave velocities were obtained on the basis of the Hamilton–Bachman method, and they served as the basis for the GADM for loose bottom sediments. The *P*–wave velocities calculated using acoustic methods are qualitatively, but not quantitatively, close to the velocities obtained by the Hamilton–Bachman method. Based on the fact that the maximum values of the longitudinal wave velocities obtained by the acoustic methods are too high, there is an error in determining the elastic properties of rocks.

The thickness of loose sediments in the GADM was determined using continuous seismic profiling [42]. In the deep part of the acoustic test site, three sedimentary layers were identified, which wedge out towards the coastline (Figure 5). The top layer of sand, 20–50 m thick near the shore, decreases to 5 m towards the open part of the bay. The second sedimentary layer is most likely composed of coarse sand with high density; the third layer consists of large boulders and pebbles filled with sand, the location of the lower boundary of which is shown in Figure 4. The shoreline in the GADM represents the limitation of the values of the acoustic parameters of loose bottom sediments, and the shore is a layer with the properties of the "Acoustic Foundation".

4.3. Acoustic Foundation

The acoustic foundation in this work is represented by igneous rocks: granites, diorites, and gabbro of the Permian age. The upper boundary of the diorite–granite Gamov complex is clearly detected, with the upper boundary submerged 20–50 m from sea level in the middle part of the bay and descending to the depth of 500 m at the exit from the bay, forming a canyon with steep slopes. The maximum immersion depth of the granite layer is 8 km from Furugelm Island, and from the side of Mount Tumannaya, this distance is about 12 km (Figure 9). The canyon at the exit from the bay forms the Tumangan synclinal zone (depression), along the sides of which separate uplifts can be traced: the Clerk anticline and the Gamov anticline. From the Gamov Peninsular in the south–west direction, a fault is detected in the granite layer. Mount Tumannaya and the Gamov anticline are structurally included in the tectonic complex of the Western Primorsky folded zone of late Paleozoic stabilization. According to geological data, on the land of the Khanka region of the Primorsky Territory of the Russian Federation, several fault zones can be traced, stretching from northwest to southeast. In addition, according to studies using magnetic prospecting, these fault zones have also been recorded on the shelf of Peter the Great Bay. They are located 7–12 km from the Gamov Peninsula, crossing the central part of the bay, and going into the open part of the sea. Faults are crushed rocks with filler–sand and interlayers of quartz. The acoustic characteristics of a fault zone differ from rocks and are highly dependent on the filler. Thus, when the filler is sand or silty component, the speed of P–waves is 1500–1900 m/s; when the filler is solid quartz veins, the speed can reach 6000 m/s. Multiple fault zones and individual shears and faults in rocks are typical geomorphological structures for the shelves of the Far Eastern seas.

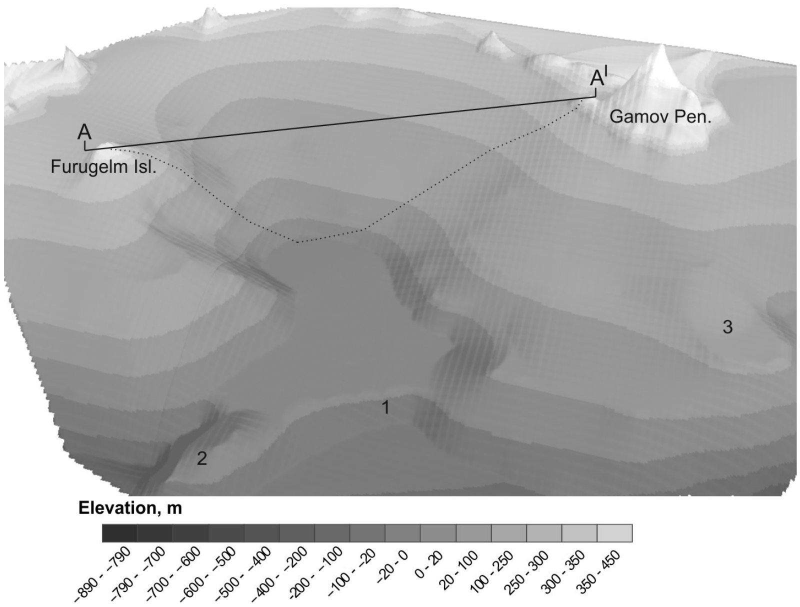

Figure 9. Restored 3D model of the acoustic foundation at the acoustic test site. The numbers show the geological structures: 1—Tumangan synclinal zone, 2—Clerk anticline, 3—Gamov anticline.

5. Conclusions

The GADM covers an area of about 800 km^2 of Peter the Great Bay (93%) and adjacent land (7%). The maximum thickness of the sedimentary layer in the GADM is 630 m. Detailing of the GADM can vary; the minimum cell size is 0.45×0.3 km and is controlled by the choice in the number of modes obtained by the SSA method for all geological layers.

Using various methods and approaches and their comparison can increase the reliability of the results. As studies in Peter the Great Bay have shown, the most realistic values of longitudinal wave velocities can be obtained on the basis of the Hamilton–Bachman method [16]. The longitudinal wave velocities calculated by acoustic methods are qualitatively close to the velocities obtained using the Hamilton–Bachman method, but quantitatively, the maximum values of the longitudinal wave velocities are overestimated by more than 200 m/s, which means that there is an error in determining the elastic properties of rocks. The work [47] notes that the Bio–Stoll method may not work correctly at high frequencies, so the error in determining the longitudinal wave velocities may be due to the use of a high-frequency emitter. In addition, the roughness of the seabed can introduce errors in measurements due to the dissipation of some of the energy. However, an important advantage of the acoustic method for determining the elastic characteristics of bottom sediments is the detailing of the measurements. It is also possible to specify zones with complex geological structures in places of bedrock outcrops and interlayering of geological layers of different composition. Therefore, the GADM uses acoustic characteristics calculated by the Hamilton–Bachman method.

Longitudinal wave velocities of the top sedimentary layer in the GADM vary from 1650 m/s to 1750 m/s. The minimum values of longitudinal wave velocities are characteristic of lowlands and the lower part of terrain folds in the area of Furugelm Island, where the area of removal and accumulation of sedimentary material by the Tumannaya River is located. Maximum values of longitudinal wave velocities are observed at underwater elevations, for example, near the Gamov Peninsula, where destruction and denudation of rocky coast occur.

The created geoacoustic digital seabed model systematizes all known geological and geophysical information about the structure of the shelf area in Peter the Great Bay. The average values of the acoustic characteristics of the object under study are presented in Table 1. In addition, the 3D GADM can be visualized on any geoinformational platform and further used in the modeling and interpretation of seismic and hydroacoustic signals on the shelf.

Detailed analysis and systematization of the available geological and geophysical data on the structure of the shelf seabed and their subsequent qualitative and quantitative formalization is an important and long-standing problem not only for the Sea of Japan but also for all Far Eastern seas. The hydrophysical test site in Peter the Great Bay provides a unique opportunity to study the oceanological and geophysical features characteristic of this region and their influence on the acoustic fields of harmonic and broadband sound sources. Clarification of the layered structure of bottom sediments' parameters and accumulation of statistical data on oceanological characteristics will allow the future to model the propagation of sound in shallow sea conditions in more detail and will also contribute to the solution of problems of tomography and construction of hydrodynamic models of shelf areas.

In different seasons, at depths of down to 70 m, the temperature of the bottom water varies from 1 to 15 °C, leading to the heating of the sedimentary layer and changes in its acoustic characteristics. The studies [48,49] investigate the temperature dependence of the acoustic parameters of the upper sediment layer. Conducting additional research on the influence of temperature on the acoustic parameters of the bottom sediments in Peter the Great Bay could allow us to make adjustments to the GADM.

Author Contributions: Conceptualization, A.S. and I.Y.; methodology, R.K.; investigation and experimental studies, A.S., I.Y. and A.K.; data curation, A.S., R.K. and A.K.; writing—original draft preparation, A.S. and R.K.; writing—review and editing, I.Y. and A.K.; visualization, R.K.; supervision, G.D.; project administration, I.Y. and G.D.; funding acquisition, G.D. All authors have read and agreed to the published version of the manuscript.

Funding: This study was supported by a grant from the Russian Science Foundation, project no. 22-17-00121, "The emergence, development and transformation of geospheric processes of the infra-sound range".

Data Availability Statement: Experimental data are archived at the Laboratory of Statistical Hydroacoustics (POI FEB RAS) and are available upon request with some restrictions applying to the availability of these data.

Acknowledgments: The authors appreciate the support of theoretical studies by the Russian State assignment, state number registration: 124022100074-9.

Conflicts of Interest: The authors declare no conflicts of interest.

References

1. Hamilton, E.L. Geoacoustic modeling of the seafloor. *J. Acoust. Soc. Am.* **1980**, *68*, 176–190. [CrossRef]
2. Brandes, H.G.; Silva, A.J.; Walter, D.J. Geo-acoustic characterization of calcareous seabed in the Florida Keys. *Mar. Geol.* **2002**, *182*, 77–102. [CrossRef]
3. Goff, J.A.; Kraftc, B.J.; Mayerc, L.A.; Schockd, S.G.; Sommerfielde, C.K.; Olsona, H.C.; Gulicka, S.P.S.; Nordfjorda, S. Seabed characterization on the New Jersey middle and outer shelf: Correlatability and spatial variability of seafloor sediment properties. *Mar. Geol.* **2004**, *209*, 147–172. [CrossRef]
4. Goff, J.A.; Austin, J.A., Jr.; Gulicka, S.; Nordfjorda, S.; Christensenb, B.; Sommerfieldc, C.; Olsona, H.; Alexanderd, C. Recent and modern marine erosion on the New Jersey outer shelf. *Mar. Geol.* **2005**, *216*, 275–296. [CrossRef]
5. Maesanoa, F.E.; D'Ambrogib, C. Vel-IO 3D: A tool for 3D velocity model construction, optimization and time-depth conversion in 3D geological modeling workflow. *Comput. Geosci.* **2017**, *99*, 171–182. [CrossRef]
6. Hampton, L. *Physics of Sound in Marine Sediments*; Plenum Press: New York, NY, USA; London, UK; Austin, TX, USA, 1974; 532p. [CrossRef]
7. Kuperman, W.A.; Jensen, F.B. *Bottom-Interacting Ocean Acoustics*; NATO Conference Series, Series IV, Marine Sciences, V. 5; Plenum Press: New York, NY, USA; London, UK, 1980. [CrossRef]
8. Zhang, W.; Xu, K.; Herke, C.; Alawneh, O.; Jafari, N.; Maiti, K.; Clower, P.O.; Glaspie, C.N.; Tupitza, J.C.; Xue, Z.G. Spatial and temporal variations of seabed sediment characteristics in the inner Louisiana shelf. *Mar. Geol.* **2023**, *463*, 107115. [CrossRef]
9. Wehra, H.; Chevrota, S.; Courriouxb, G.; Guillenb, A. A three-dimensional model of the Pyrenees and their foreland basins from geological and gravimetric data. *Tectonophysics* **2018**, *734–735*, 16–32. [CrossRef]
10. Unnithan, S.L.K.; Biswal, B.; Sharples, W.; Rüdiger, C.; Bahramian, K.; Hou, J. Sensitivity Analysis of Modelled Flood Inundation Extents over Hawkesbury–Nepean Catchment. *Geosciences* **2023**, *13*, 67. [CrossRef]
11. Lynn, H.; Chen, P.; Hu, C. High-dimensionality 3D seismic data visualization and interpretation: Simultaneous interpretation of nine co-rendered volumes. *Recorder* **2003**, *28*, 1–8. Available online: https://csegrecorder.com/articles/view/high-dimensionality-3d-seismic-data-visualization-and-interpretation (accessed on 15 August 2024).
12. Maxelon, M.; Renard, P.; Courrioux, G.; Brandli, M.; Mancktelowa, N. A work flow to facilitate three-dimensional geometrical modelling of complexpol y-deformed geological units. *Comput. Geosci.* **2009**, *35*, 644–658. [CrossRef]
13. Fengqin, Z.; Gulin, O.E.; Yaroshchuk, I.O. Average intensity of low-frequency sound and its fluctuations in a shallow sea with a range-dependent random impedance of the liquid bottom. *Appl. Sci.* **2021**, *11*, 11575. [CrossRef]
14. Gulin, O.E.; Yaroshchuk, I.O. On average losses of low-frequernce sound in a two-dimensional shallow-water random waveguide. *J. Mar. Sci. Eng.* **2022**, *10*, 822. [CrossRef]
15. Pivovarov, A.A.; Yaroshchuk, I.O.; Dolgikh, G.I.; Shvyrev, A.N.; Samchenko, A.N. An Autonomous Acoustic Logger and Its Application as Part of a Hydrophysical Complex. *Instrum. Exp. Tech.* **2021**, *64*, 468–473. [CrossRef]
16. Hamilton, E.L.; Bachman, R.T. Sound velocity and related properties of marine sediments. *J. Acoust. Soc. Am.* **1982**, *72*, 1891–1904. [CrossRef]
17. Nikolova, V.; Gospodinova, V.; Kamburov, A. Assessment of Unmanned Aerial System Flight Plans for Data Acquisition from Erosional Terrain. *Geosciences* **2024**, *14*, 75. [CrossRef]
18. Kakavas, M.P.; Frattini, P.; Previati, A.; Nikolakopoulos, K.G. Evaluating the Impact of DEM Spatial Resolution on 3D Rockfall Simulation in GIS Environment. *Geosciences* **2024**, *14*, 200. [CrossRef]
19. Sibson, R. A brief description of natural neighbor interpolation (Chapter 2). In *Interpreting Multivariate Data*; Barnett, V., Ed.; John Wiley: New York, NY, USA; Chichester, UK, 1981; pp. 21–36. [CrossRef]
20. Golyandina, N.E.; Usevich, K.D.; Florinsky, I.V. Filtering of Digital Terrain Models by Two Dimensional Singular Spectrum Analysis. *Int. J. Ecol. Dev.* **2007**, *8*, 81–94. Available online: https://www.researchgate.net/publication/254469642 (accessed on 15 August 2024).

21. Navarra, A.; Simoncini, V. *A Guide to Empirical Orthogonal Functions for Climate Data Analisis*; Springer: Berlin/Heidelberg, Germany, 2010; Volume 152. [CrossRef]
22. Biot, M.A. Theory of propagation of elastic waves in fluid-saturated porous solid: II High frequency range, distributions. *J. Acoust. Soc. Am.* **1956**, *83*, 1744–1751. [CrossRef]
23. Biot, M.A. Mechanics of deformation and acoustic propagation in porous media. *J. Appl. Phys.* **1962**, *33*, 1482–1498. [CrossRef]
24. Stoll, R.D. Acoustic waves in saturated sediments. In *Physics of Sound in Marine Sediments*; Hampton, L., Ed.; Springer: New York, NY, USA, 1974; pp. 19–39. [CrossRef]
25. Buchanan, J.L. *An Assessment of the Biot-Stoll Model of a Poroelastic Seabed*; Mathematics Department, U.S. Naval Academy: Annapolis, MD, USA, 2005; pp. 21402–25002. Available online: https://archive.org/details/DTIC_ADA437036 (accessed on 15 August 2024).
26. Ding, H.; Xu, S.; Xu, C.; Tong, L.; Jiang, Y.; Lei, Z. Influence factors on the nonlocal parameter and scale factor in strain gradient nonlocal Biot theory. *Soil Dyn. Earthq. Eng.* **2023**, *166*, 107779. [CrossRef]
27. Richardson, M.D.; Lavoie, D.L.; Briggs, K.B. Geoacoustic and physical properties of carbonate sediments of the Lower Florida Keys. *Geo-Mar. Lett.* **1997**, *17*, 316–324. [CrossRef]
28. Amiri-Simkooei, A.R.; Koop, L.; van der Reijden, K.J.; Snellen, M.; Simons, D.G. Seafloor Characterization Using Multibeam Echosounder Backscatter Data: Methodology and Results in the North Sea. *Geosciences* **2019**, *9*, 292. [CrossRef]
29. Santos, R.; Rodrigues, A.; Quartau, R. Acoustic remote characterization of seabed sediments using the Angular Range Analysis technique: The inlet channel of Tagus River estuary (Portugal). *Mar. Geol.* **2018**, *400*, 60–75. [CrossRef]
30. Schimel, A.C.G.; Ierodiaconou, D.; Hulands, L.; Kennedy, D.M. Accounting for uncertainty in volumes of seabed change measured with repeat multibeam sonar surveys. *Cont. Shelf Res.* **2015**, *111*, 52–68. [CrossRef]
31. Lisyutin, V.A.; Lastovenko, O.R. Evaluation of the effect of internal and viscous friction on the dispersion and attenuation of sound in unconsolidated marine sediments. *Acoust. J.* **2020**, *66*, 420–436. [CrossRef]
32. Dolgikh, G.; Dolgikh, S.; Chupin, V.; Davydov, A.; Mishakov, A. Remote Seismoacoustic Monitoring of Tropical Cyclones in the Sea of Japan. *Remote Sens.* **2023**, *15*, 1707. [CrossRef]
33. Pivovarov, A.A.; Yaroshchuk, I.O.; Shvyrev, A.N.; Samchenko, A.N. An Autonomous Low-Frequency Broadb and Hydroacoustic Emitting Station with an Electromagnetic Transducer. *Instrum. Exp. Tech.* **2020**, *63*, 880–884. [CrossRef]
34. Karnaukh, V.N.; Astakhov, A.S.; Vereshchagina, O.F.; Tsoy, I.B.; Kosmach, D.A.; Sagalaev, S.G.; Volkova, T.I.; Dubina, V.A.; Prushkovskaya, I.A. Formation of subsurface shallow gas accumulations in Amurskiy Bay (Peter the Great Bay, Sea of Japan) as a result of postglacial sea-level change, paleoceanographic conditions and hydrological activity. *Mar. Geol.* **2016**, *372*, 31–52. [CrossRef]
35. Licht, F.R.; Astakhov, A.S.; Botsul, A.I.; Derkachev, A.N.; Dudarev, O.V.; Markov, Y.D.; Utkin, I.V. *Sediment Structure and Facies of the SEA of Japan*; DVNTs of the USSR Academy of Sciences: Vladivostok, Russia, 1983; 286p. (In Russian)
36. Markov, Y.D. *The South Sea shelf of the Sea of Japan in the Late Pleistocene and Holocene*; DVNTs of the USSR Academy of Sciences: Vladivostok, Russia, 1983; 128p. (In Russian)
37. Hamilton, E.L. Vp/Vs and Poisson's Ratios in Marine Sediments and Rocks. *J. Acoust. Soc. Am.* **1979**, *66*, 1093–1101. [CrossRef]
38. Hamilton, E.L. Variation of Density and Porosity with Depth in Deep-Sea Sediments. *J. Sediment. Petrol.* **1976**, *46*, 280–300. [CrossRef]
39. Hamilton, E.L. Sound Velocity as a Function of Depth in Marine Sediments. *J. Acoust. Soc. Am.* **1985**, *78*, 1348–1355. [CrossRef]
40. Samchenko, A.; Dolgikh, G.; Yaroshchuk, I.; Kosheleva, A.; Pivovarov, A.; Novotryasov, V. Extreme Hydrometeorological Conditions of Sediment Waves' Formation and Migration in Peter the Great Bay (The Sea of Japan). *Water* **2023**, *15*, 393. [CrossRef]
41. Yaroshchuk, I.; Kosheleva, A.; Lazaryuk, A.; Dolgikh, G.; Pivovarov, A.; Samchenko, A.; Shvyrev, A.; Gulin, O.; Korotchenko, R. Estimation of Seawater Hydrophysical Characteristics from Thermistor Strings and CTD Data in the Sea of Japan Shelf Zone. *J. Mar. Sci. Eng.* **2023**, *11*, 1204. [CrossRef]
42. Samchenko, A.N.; Karnaukh, V.N.; Aksentov, K.I. Geological-geophysical studies of the upper sedimentary cover and geoacoustic model for the Posiet Bay shelf (the Sea of Japan). *Russ. J. Pac. Geol.* **2013**, *32*, 65–74. Available online: https://www.elibrary.ru/download/elibrary_19062966_22557046.pdf (accessed on 15 August 2024). (In Russian).
43. Karnaukh, V.N.; Karp, B.Y.; Tsoy, I.B. Seismostratigraphy and sedimentation environment on the shelf and continental slope of Peter the Great Bay (Sea of Japan). *Oceanology* **2007**, *47*, 691–704. [CrossRef]
44. Robb, G.B.N.; Best, A.I.; Dix, J.K.; Bull, J.; Leighton, M.T.G.; White, P.R. The frequency dependence of compressional wave velocity and attenuation coefficient of intertidal marine sediments. *J. Acoust. Soc. Am.* **2006**, *120*, 2526–2537. [CrossRef]
45. Williams, K.L. An effective density fluid model for acoustic propagation in sediments derived from Biot theory. *J. Acoust. Soc. Am.* **2001**, *110*, 2276–2281. [CrossRef]
46. Schock, S.G. Method for estimating the physical and acoustic properties of the sea bed using chirp sonar data. *IEEE J. Ocean. Eng.* **2004**, *29*, 1200–1217. [CrossRef]
47. Schock, S.G. Remote estimates of physical and acoustic sediment properties in the South China Sea using chirp sonar data and the Biot model. *IEEE J. Ocean. Eng.* **2004**, *29*, 1218–1230. [CrossRef]

48. Yusupov, V.; Salomatin, A.; Shakhova, N.; Chernykh, D.; Domaniuk, A.; Semiletov, I. Echo Sounding for Remote Estimation of Seabed Temperatures on the Arctic Shelf. *Geosciences* **2022**, *12*, 315. [CrossRef]
49. Yusupov, V.I.; Semiletov, I.P.; Chernykh, D.V.; Salomatin, A.S. Active High-Frequency Acoustic Thermometry of Frozen Water-Saturated Media. *Acoust. Phys.* **2022**, *68*, 459–466. [CrossRef]